

Ab initio study of magnetic structure and exchange coupling in Co₂MnSi/Cr/Co₂MnSi trilayersW. Kakeno,¹ S. Honda,^{1,*} H. Itoh,² and J. Inoue^{1,†}¹*Department of Applied Physics, Nagoya University, Nagoya 464-8603, Japan*²*Department of Pure and Applied Physics, Kansai University, Suita 564-8680, Japan*

(Received 3 March 2010; revised manuscript received 28 May 2010; published 14 July 2010)

The electronic and magnetic structures and magnetic moments of Co₂MnSi (CMS)/Cr/Co₂MnSi (001) trilayers are calculated by the first-principles method and compared to those calculated for Fe/Cr/Fe trilayers. The magnetic moments of Co are found to be parallel to those of Cr, whereas those of Mn are antiparallel to Cr moments. The results suggest that an antiphase structure in CMS layers may also bring about a frustration in the interlayer exchange coupling in multilayers. We also study the effects of antisite atoms at interfaces on the electronic and magnetic structures and find that the antiferromagnetic ordering of Cr moments is more robust than that in Fe/Cr/Fe trilayers. We propose a possible scenario in which the robustness of the antiferromagnetic ordering of Cr moments and the frustration in the interlayer exchange coupling, which is caused by antiphase or step structures, are responsible for the biquadratic coupling observed in CMS/Cr multilayers.

DOI: [10.1103/PhysRevB.82.014413](https://doi.org/10.1103/PhysRevB.82.014413)

PACS number(s): 75.70.Cn, 73.20.At, 73.21.Ac

I. INTRODUCTION

Spintronics has developed into a rich field of science and technology following the discovery of giant magnetoresistance and tunnel magnetoresistance (GMR and TMR) (Refs. 1–3) and current-induced magnetization switching (CIMS).⁴ Magnetoresistive sensors using GMR and TMR are already in wide commercial use, and magnetoresistive random access memory using CIMS is currently under investigation for technological applications. High spin polarization of current through ferromagnetic junctions is desirable in these phenomena. Therefore, half metals that show 100% spin polarization attract much interest for use in ferromagnetic junctions. Among many half metals, Heusler alloys have been used for TMR junctions because they have high Curie temperatures and show good lattice matching with MgO barriers.^{5,6} Magnetic multilayers using Heusler alloys are also promising materials for technological applications because they may produce a high GMR ratio, especially in the current-perpendicular-to-plane geometry.

A key phenomenon in GMR is interlayer exchange coupling (IEC) (Refs. 1, 2, and 7) between ferromagnetic layers separated by a nonmagnetic layer. The coupling energy produced by IEC in ferromagnetic multilayers is usually described in terms of bilinear coupling J_1 and biquadratic coupling J_2 as

$$E_{\text{ex}} = -J_1 \cos \theta - J_2 \cos^2 \theta, \quad (1)$$

where θ is the relative angle between two magnetizations. So far, many experimental and theoretical studies evaluated the values of J_1 and J_2 and clarified the origin of IEC.^{8–11} In many multilayers, $|J_1| \gg |J_2|$, and J_1 show a long-period oscillation as a function of the nonmagnetic layer's thickness. The long-period oscillation of J_1 has been attributed to spanning wave vectors on the Fermi surface of the nonmagnetic metal.^{12–14} A short-period oscillation was also observed for clean samples.^{15,16} In some multilayers, such as Fe/Al and Fe/Au as well as Fe/Cr $|J_2|$ is the same order of magnitude as $|J_1|$.^{17–20} When the biquadratic coupling exceeds the bilinear

coupling, 90° coupling of the magnetization of the ferromagnetic layers appears.

Recently, IEC in Co₂MnSi (CMS)/Cr multilayers has been measured. The following results were reported:^{21–25} CMS/Cr multilayers show dominant 90° coupling; that is, $|J_2| \gg J_1 \sim 0$, $|J_2|$ decreases with increasing Co content in CMS, the 90° coupling is well correlated with the B2 structure of Co₂FeSi, and the 90° coupling disappears in CMS/V multilayers.

Several mechanisms have been proposed so far for the 90° coupling:^{26–28} an intrinsic mechanism, a model of J_1 fluctuation due to interfacial roughness, a loose spin model, a dipole-dipole interaction, and a proximity model that is applicable to antiferromagnetic spacer layers. However, none of these mechanisms can explain the observed results for Fe/Al, Fe/Au, and Fe/Cr multilayers in a unified way, and the mechanism of the 90° coupling is still controversial. The origin of the 90° coupling in CMS/Cr multilayers also remains to be explained.

In this paper, we perform first-principles band calculations for CMS/Cr/CMS trilayers (TLs), and calculate the electronic structure and magnetic moment of each element of CMS and the coupling energy. We also study the effects of antisite atoms at interfaces on the magnetic structure and coupling energy by using a supercell structure. Comparing the results with those calculated for Fe/Cr/Fe TLs by the same method, we propose a possible origin of the 90° coupling in CMS/Cr multilayers.

The paper is organized as follows. In the next section, we briefly explain the model and the method of calculation. Calculated results are presented in Sec. III. In Sec. III A, we show the results for Fe/Cr/Fe and Fe/V/Fe TLs which are compared with previous results reported for first-principles or tight-binding calculations, and in the next section we present results for CMS/Cr/CMS TLs with collinear alignment of CMS magnetizations. We also present calculated results of the magnetic structures of Fe/Cr/Fe and CMS/Cr/CMS TLs with interfaces at which antisite atoms exist. Section IV discusses the difference between the magnetic structures in Fe/Cr and CMS/Cr multilayers and a possible

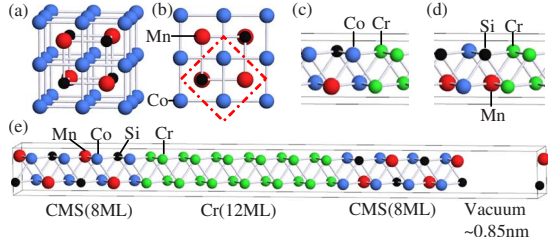


FIG. 1. (Color online) (a) Lattice structure of CMS, (b) structure projected on the [001] plane, arrangement of atoms near CMS/Cr interface with (c) (Co-Co)/Cr contact and (d) (Mn-Si)/Cr contact, and (e) unit cell of CMS/Cr/CMS/vacuum used for the calculation. The cross section of the super cell is shown in (b) as an area enclosed by chained lines.

mechanism for the observed 90° coupling in CMS/Cr multilayers. Conclusions are given in the final section.

II. MODELS AND METHOD OF CALCULATION

We prepare a superlattice of CMS (8 ML)/Cr (12 ML)/CMS (8 ML)/vacuum (0.85 nm) stacked along the (001) direction as a typical structure for CMS/Cr/CMS TLs. (ML stands for monolayer.) The lattice structure of CMS is shown in Fig. 1(a). The lattice constant of the CMS lattice is 0.3995 nm, slightly shorter than that of Cr, which has a lattice constant of 0.4080 nm. In the calculations, we adopt the lattice constant of CMS for the CMS/Cr/CMS TL since the total energy of the system calculated with the CMS lattice constant was lower than that of the Cr lattice constant. The lattice mismatch of 2.1% has thus been neglected. The lattice structure projected to the [001] plane of the CMS lattice is shown in Fig. 1(b); the area enclosed by chained lines is the cross section of the supercell used in the calculations. The arrangements of atoms near the interface are shown in Figs. 1(c) and 1(d). The supercell structure used for the first-principles calculations is shown in Fig. 1(e). A unit cell contains 56 atoms. We see that (Co-Co) and (Mn-Si) layers are stacked alternately in the superlattice of the CMS layer. Therefore, the CMS/Cr interface can feature either (Co-Co)/Cr contact or (Mn-Si)/Cr contact; as a result, CMS/Cr/CMS trilayers have three different interface combinations. The position of Cr atoms is taken to be the $(\pm 1, \pm 1, 1)$ direction from the atomic positions of CMS, and the lattice spacing between CMS and Cr is assumed to be the same as the CMS lattice constant.

We use the first-principles band calculation given by the VASP package, in which the projector augmented wave (PAW) pseudopotential method and a spin-polarized generalized gradient approximation-PW (Perdew-Wang) method are adopted. The cutoff of the plane waves is 270 eV and the k -point sampling is (5,5,5). The total energy, electronic structure, and magnetic moment of each atom are calculated for parallel (P) and antiparallel (AP) alignments of the magnetization in the ferromagnetic layers. The difference in total energy between P and AP alignments is defined as $\Delta E = E_{AP} - E_P$. When $\Delta E > 0 (< 0)$, the P (AP) alignment is stable.

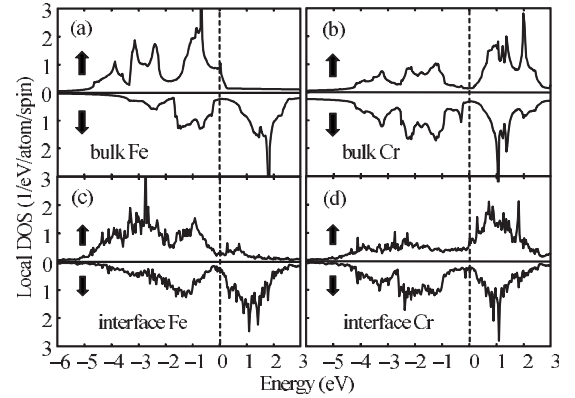


FIG. 2. Calculated results of the DOS of (a) ferromagnetic bulk Fe and (b) antiferromagnetic bulk Cr. (c) and (d) show the local DOS of Fe and Cr, respectively, at the interface in an Fe/Cr/Fe TL. Arrows indicate spins and a vertical dotted line shows the Fermi energy.

We perform calculations for three types of CMS/Cr/CMS TLs: TLs with (Co-Co)/Cr contact for both interfaces, those with (Mn-Si)/Cr contact for both interfaces, and those with (Co-Co)/Cr contact for one interface and (Mn-Si)/Cr contact for the other interface. We further study the effects of antisite atoms at the interfaces. This is possible because the cross section of the superlattice contains two atoms, as shown in Figs. 1(c) and 1(d). Hereafter, we denote an antisite atom A that replaces a B atom as $A(B)$ or A^* in the tables and figures. In addition to CMS/Cr/CMS TLs, we also perform the same kind of calculations for Fe/Cr/Fe as well as Fe/V/Fe and CMS/V/CMS TLs because experimental group reported results for CMS/V/CMS multilayers.²⁹ The results are then compared to those calculated for CMS/Cr/CMS TLs. We basically assume a collinear alignment of Fe and CMS magnetization for the Fe/Cr/Fe and CMS/Cr/CMS TLs, respectively.

III. CALCULATED RESULTS

A. Fe/Cr/Fe and Fe/V/Fe TLs

Figures 2(a) and 2(b) show the density of states (DOS) of ferromagnetic bulk Fe and antiferromagnetic bulk Cr, respectively. The local DOSs of Fe and Cr at the interface of an Fe(8 ML)/Cr(12 ML)/Fe(8 ML) TL with a collinear magnetization alignment are presented in Figs. 2(c) and 2(d), respectively. We see that the up-spin local DOSs of Fe and Cr are strongly modified by band mixing between Fe and Cr at the interface. On the other hand, the down-spin DOSs of Fe and Cr are almost unchanged. Note that the up-spin and down-spin DOSs of Cr are not symmetrical because a simple antiferromagnetic state is assumed for bulk Cr.

The magnetic moments and magnetic structures of AP and P alignments calculated for an Fe(8 ML)/Cr(12 ML)/Fe(8 ML) TL are shown in Figs. 3(a) and 3(b), respectively. Since the number of Cr MLs is even, the Cr layer is ordered antiferromagnetically in the AP alignment, as Fig. 3(a) shows. In contrast, in the P alignment, Cr moments cannot be well ordered antiferromagnetically and are shrank, as Fig. 3(b)

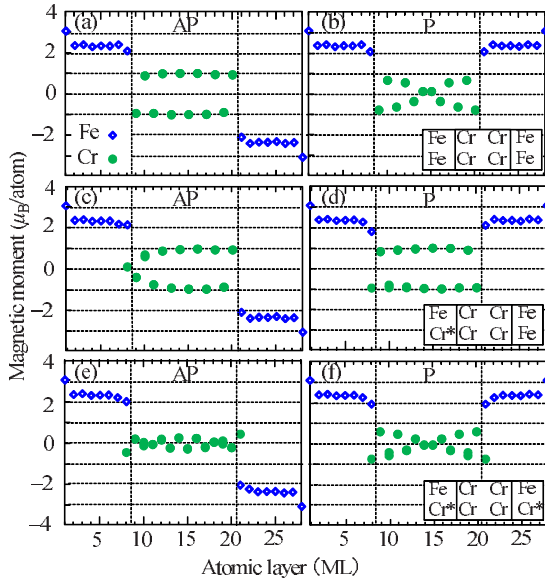


FIG. 3. (Color online) Calculated results of the magnetic structures of an Fe(8 ML)/Cr(12 ML)/Fe(8 ML) TL with (a) AP and (b) P alignments of Fe magnetization, those of an Fe/Cr/Fe TL with (c) AP and (d) P alignments with one antisite Cr(Fe) atom at one interface, and those of an Fe/Cr/Fe TL with (e) AP and (f) P alignments with one antisite Cr(Fe) atom at each interface. Insets show the type of contact at the interface. (a), (d), and (f) show the stable alignment of Fe magnetization. Elements marked with * indicate antisite atoms at the interface.

shows. At the interface, the Fe moment m_{Fe} is antiparallel to the Cr moment m_{Cr} . Absolute values of m_{Fe} and m_{Cr} are $2.2 \mu_{\text{B}}/\text{atom}$ and $\sim 1 \mu_{\text{B}}/\text{atom}$, respectively, in the AP alignment. The value of m_{Fe} increases to $\sim 3 \mu_{\text{B}}/\text{atom}$ at the surface. As a result, the stable alignment changes layer by layer with increasing Cr thickness. These results agree qualitatively with previous ones,^{14,30–34} however, quantitative agreement/disagreement needs discussions.

The coupling energy $\Delta E \sim -209 \text{ erg}/\text{cm}^2$ is much larger than the measured value for IEC. It is even larger than those calculated previously by a factor 4.^{31,33} We may attribute the latter difference to rather large values of m_{Cr} as compared with those calculated previously. Our results of m_{Cr} are about $1 \mu_{\text{B}}$ for the stable AP alignment with 12 Cr atomic layers. In the P alignment, on the other hand, they shrink to smaller values due to a mismatching of the antiferromagnetic ordering in Cr layer with Fe magnetization. Calculated values of m_{Cr} by Stoeffler-Gautier³¹ and Mirbt *et al.*³³ are about $0.6 \mu_{\text{B}}$ and $0.3 \mu_{\text{B}}$ per atom, respectively. Since the calculated energy of trilayers includes the magnetic energy of Cr layers, ΔE should include the energy change caused by the shrinkage of m_{Cr} . At the moment, however, we do not understand the reason for different values of m_{Cr} calculated by three groups.

Calculated results of ΔE for Fe/V/Fe TLs may give some more information on the exchange coupling calculated in this kind of the method. We performed detailed calculation of the electronic and magnetic states and ΔE for Fe/V/Fe TLs by adopting several k -point samplings, (15, 15, 5), (21, 21, 5), and (25, 25, 5). We found that the magnitude of ΔE and m_{V}

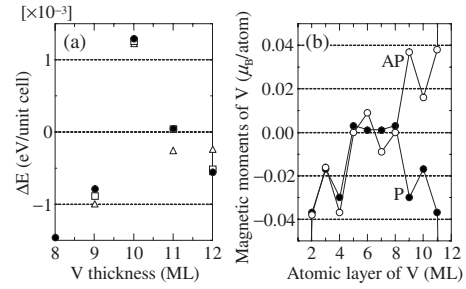


FIG. 4. Calculated results of (a) ΔE in Fe/V/Fe as a function of V thickness for several k -point samplings, triangles: (15, 15, 5), squares: (21, 21, 5), and closed circles: (25, 25, 5), and (b) magnetic moments of V atoms in an Fe/V(12 ML)/Fe TL. Absolute values of m_{V} at the first and 12th V layers are $0.468 \mu_{\text{B}}$ and $0.469 \mu_{\text{B}}$ per atom for P and AP alignments, respectively.

are smaller than those in Fe/Cr/Fe TLs by two and one order magnitude, respectively, as shown in Fig. 4. We see in Fig. 4(a) that the value of ΔE is about $0.5 \text{ meV}/\text{unit cell}$ (about $1 \text{ erg}/\text{cm}^2$) for an Fe(8 ML)/V(12 ML)/Fe(8 ML) TL, which, however, is still larger than the experimental values of Fe/V multilayers by one order of magnitude.³⁵ The difference between calculated and experimental values of ΔE might also be attributed a change in m_{V} in the central region of V layer as shown in the Fig. 4(b). The overall reduction in m_{V} by a factor 10 as compared with m_{Cr} might result in a smaller value of ΔE in Fe/V/Fe TLs than that in Fe/Cr/Fe TLs by two orders of magnitude. Thus the contribution of magnetic energy in the spacer metals seems to be large in the calculations. It may be interesting to note that the variation in m_{V} in the V layer is different from either RKKY type oscillation or a simple alternate oscillation calculated for Fe/Cr/Fe TLs. As shown in Fig. 4(a), the numerical accuracy of ΔE may not be insufficient. However, the accuracy should be confirmed by performing extended calculation for thicker V layers, which will be a future problem due to time consuming calculation.

We also calculated the magnetic structure for an Fe(8 ML)/Cr(24 ML)/Fe(8 ML) TL with a collinear alignment of Fe magnetizations and found that a spin-density wave structure is realized, which is consistent with previous reports.^{36–38}

Since we prepared a large unit cell, the cross section of which contains two Fe or Cr atoms, it is possible to study the effects of antisite atoms at the interface on the magnetic structure and IEC. The magnetic structures for an Fe/Cr/Fe TL with an antisite Cr(Fe) at one interface are shown in Figs. 3(c) and 3(d) for AP and P alignments, respectively. Antisite atoms make ΔE positive and stabilize the P alignment. As Fig. 3(c) shows, shrinkage in Cr moments appears with AP alignment, whereas those in P alignment show an antiferromagnetic ordering, as Fig. 3(d) shows. When antisite atoms exist at both interfaces, the shrinkage in Cr moments becomes even larger, as shown in Figs. 3(e) and 3(f) for AP and P alignments, respectively. We also find that the magnitude of ΔE decreases substantially, as shown in Table I. We may attribute the shrinkage of the Cr moments and the reduction in ΔE to a frustration of magnetic alignment at the interface. It is noted that two Cr sites in the unit cell are no more

TABLE I. Stable magnetization alignment and values of ΔE for Fe/Cr/Fe trilayers with different interfaces. Elements marked with * indicate antisite atoms at the interface.

Interface	Stable alignment	ΔE (erg/cm ²)
(Fe-Fe)/Cr/(Fe-Fe)	AP	-209.0
(Fe-Cr [*])/Cr/(Fe-Fe)	P	69.4
(Fe-Cr [*])/Cr/(Fe-Cr [*])	P	28.6

equivalent when antisite atoms exist at the interface. The difference in m_{Cr} on the nonequivalent sites, however, is fairly small.

B. CMS/Cr/CMS TLs

The calculated DOS of bulk CMS is shown in Fig. 5. The DOS shows half metallicity, and the total magnetization is 5 μ_B per unit cell of Co₂MnSi, as expected.

Figure 6 shows the local DOSs of CMS(8 ML)/Cr(12 ML)/CMS(8 ML) TLs with a collinear magnetization alignment. The local DOSs of Co and Mn atoms in the interior region of the TL are shown in Figs. 6(a) and 6(b), respectively. We find that half metallicity is well preserved in the interior region. However, the half-metallic character is nearly lost for Co and Mn atoms at the interface, as shown in Figs. 6(c) and 6(e), respectively. This is attributed to band mixing between the CMS and Cr layers.

Calculated results of the magnetic moments and magnetic structures for CMS(8 ML)/Cr(12 ML)/CMS(8 ML) TLs with perfect interfaces are shown in Figs. 7(a)–7(f). As mentioned, three combinations of (Co-Co)/Cr and (Mn-Si)/Cr contacts are possible in a TL. Figures 7(a) and 7(b) show the magnetic moments for AP and P alignments, respectively, of a TL in which both interfaces consist of (Co-Co)/Cr contacts. Since the number of Cr MLs is even, Cr moments show antiferromagnetic ordering in the AP alignment. In the P alignment, on the other hand, Cr moments shrink, making that alignment unstable. The Mn, Co, and Cr moments in the AP alignment are obtained as $m_{Mn} \approx 3 \mu_B/\text{atom}$, $m_{Co} \approx 1 \mu_B/\text{atom}$, and $m_{Cr} \approx 0.7 \mu_B/\text{atom}$, and m_{Co} and m_{Cr} are parallel at the interface. The results for Cr moments are quite

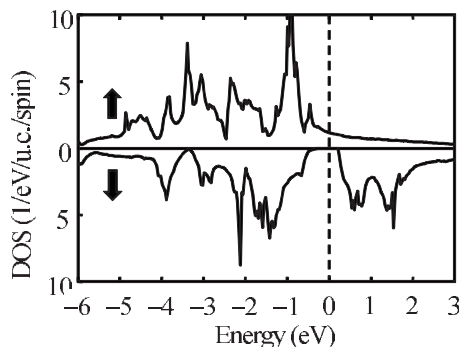


FIG. 5. Calculated total DOS of bulk Co₂MnSi. Arrows indicate the spins and a vertical dotted line shows the Fermi level.

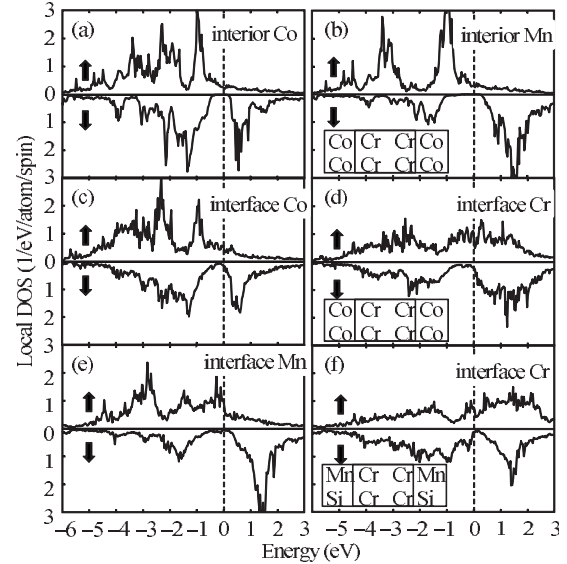


FIG. 6. Calculated DOS of a CMS/Cr/CMS TL in AP alignment: local DOSs of (a) an interior Co, (b) an interior Mn, (c) an interface Co, and (d) an interface Cr in a TL with (Co-Co)/Cr contacts at both interfaces, and local DOSs of (e) an interface Mn and (f) an interface Cr for a TL with (Mn-Si)/Cr contact at both interfaces. Insets show the type of contact at the interface.

similar to those in Fe/Cr/Fe TLs. The enhancement of m_{Mn} at the surface of the TL is attributed to a surface effect. It is also noted that two Cr sites in the unit cell are no more equivalent in CMS/Cr/CMS TLs. The difference in m_{Cr} on the nonequivalent sites is fairly small as shown in the figure.

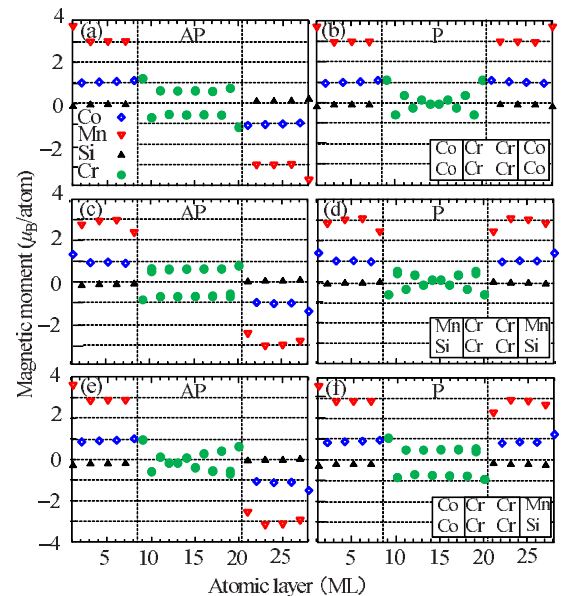


FIG. 7. (Color online) Calculated magnetic structures of CMS/Cr(12 ML)/CMS TLs with AP and P alignments of CMS magnetization: (a) and (b) results for a TL with (Co-Co)/Cr contact at both interfaces, (c) and (d) those for a TL with (Mn-Si)/Cr contact at both interfaces, and (e) and (f) those for a TL with (Co-Co)/Cr contact for one interface and (Mn-Si)/Cr contact for the other. Insets show the type of contact at the interfaces.

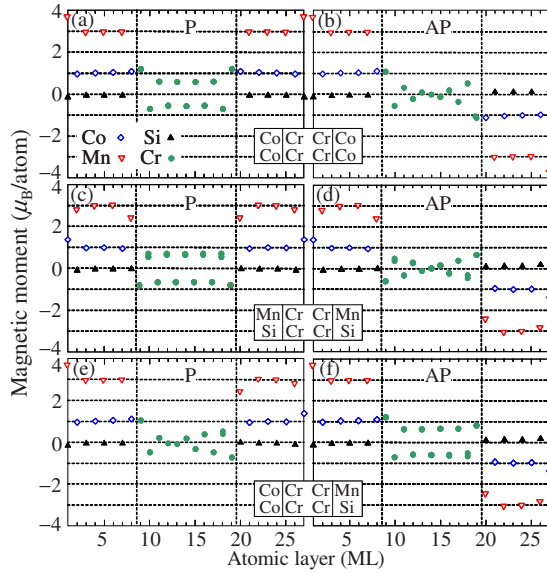


FIG. 8. (Color online) Calculated results of the magnetic structures of an CMS/Cr(11 ML)/CMS TL with AP and P alignments of CMS magnetization: (a) and (b) results for a TL with (Co-Co)/Cr contact at both interfaces, (c) and (d) those for a TL with (Mn-Si)/Cr contact at both interfaces, and (e) and (f) those for a TL with (Co-Co)/Cr contact for one interface and (Mn-Si)/Cr contact for the other. Insets show the type of contact at the interfaces.

The magnetic moments and magnetic structures calculated for a TL with (Mn-Si)/Cr contacts are shown in Figs. 7(c) and 7(d) for AP and P alignments, respectively. The results are quite similar to those obtained for the TL with (Co-Co)/Cr contacts, except that the alignment of m_{Mn} and m_{Cr} is AP, and m_{Mn} is slightly reduced to $\sim 2.5 \mu_{\text{B}}/\text{atom}$ at the interface. Results for a TL with interfaces formed by (Co-Co)/Cr and (Mn-Si)/Cr contacts are shown in Figs. 7(e) and 7(f) for AP and P alignments, respectively. We find that Cr moments are ordered antiferromagnetically in the P alignment and shrank in the AP alignment. As a result, the P alignment becomes stable in this case. This is because m_{Cr} is parallel to m_{Co} at the (Co-Co)/Cr contact and antiparallel to m_{Mn} at the other contact. This is a characteristic feature of CMS/Cr/CMS TLs in which two types of magnetic atoms are included in the ferromagnetic layers.

Because Cr layer tends to order antiferromagnetically, P and AP alignments of CMS magnetization appear alternately with increasing Cr thickness. To show this clearly, we present calculated results of CMS/Cr(11 ML)/CMS TLs in Fig. 8. For odd number of Cr atomic layer, P alignment of CMS magnetization is stable for the same type contact at both interfaces while AP alignment is stable for different types of contact at two interfaces of TLs. This is in contrast to the stable alignment for TLs with even number of Cr atomic layers.

We also performed the calculation for a CMS/V/CMS/vacuum superlattice and compared the results with experimental ones.²⁹ We found that the result is nearly the same as that obtained for Fe/V/Fe. Thus, the antiferromagnetic structure of Cr layer is important in IEC in CMS/Cr/CMS TLs as well as in Fe/Cr/Fe TLs.

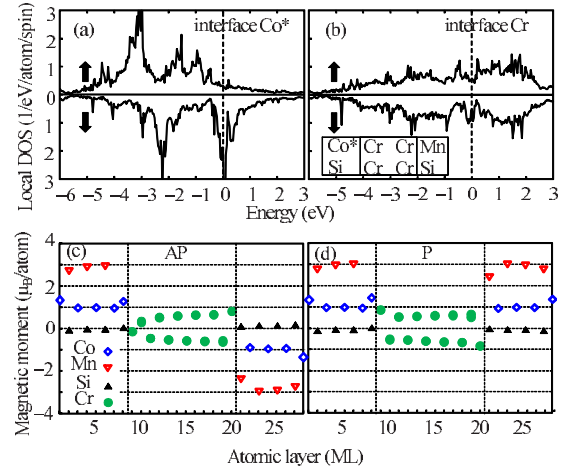


FIG. 9. (Color online) Calculated local DOSs of (a) an interface Co and (b) an interface Cr in a CMS/Cr/CMS TL with an antisite Co(Mn) at one interface, and corresponding results of magnetic moments in (c) AP and (d) P alignments. Elements marked with * are antisite atoms.

Since CMS includes three different atoms, much variety is possible in antisite structures at the interfaces in CMS/Cr/CMS TLs. To study the effects of roughness at the interfaces on the electronic and magnetic structures, we perform the calculations for CMS/Cr/CMS TLs with antisite atoms at the interface.

The local DOSs of Co(Mn) and Cr at an interface with an antisite Co(Mn) atom are shown in Figs. 9(a) and 9(b), respectively. The half metallicity vanishes completely and a rather high DOS appears at the Fermi energy. The high DOS appearing in the energy-gap region is attributed to in-gap states rather than to band mixing at the interface. The results agree qualitatively with previous first-principles calculations for antisite Co in a bulk CMS.^{39,40}

The corresponding magnetic moments and magnetic structures are shown in Figs. 9(c) and 9(d) for AP and P alignments, respectively. Cr moments are antiferromagnetically ordered in the stable P alignment. On the other hand, in the unstable AP alignment, some Cr moments become small near the antisite atom interface. This is attributed to a change in the direction of the magnetic moment of the antisite atom; the Co(Mn) moment is parallel to the Cr moment, whereas the Mn moment is antiparallel to the Cr moment.

In Table II, we summarize the calculated results of a stable alignment of CMS magnetization and the values of ΔE for CMS(8 ML)/Cr(12 ML)/CMS(8 ML) TLs with perfect interfaces and those with antisite atoms at interfaces. Despite a few exceptions, we find that the P alignment tends to be stable in a combination of (Co-Co)/Cr and (Mn-Si)/Cr interfaces, and that the AP alignment is stable in the other combinations of interfaces regardless of the presence of antisite atoms at the interface. The result is attributed to the AP alignment between m_{Mn} and m_{Cr} and the P alignment between m_{Co} and m_{Cr} . We also found that antisite Co(Cr) atoms have the same tendency (not shown). Note that ΔE , and thus the magnetization alignment, are less affected by antisite atoms in CMS/Cr/CMS TLs than in Fe/Cr/Fe TLs. The result contrasts noticeably with that obtained for Fe/Cr/Fe TLs shown in Table I.

TABLE II. Calculated results of the stable magnetization alignment and values of ΔE for CMS(8 ML)/Cr(12 ML)/CMS(8 ML) TLs with perfect interfaces and those with antisite atoms at one interface. Elements marked with * are antisite atoms.

Interface	Stable alignment	ΔE (erg/cm ²)
(Co-Co)/Cr/(Co-Co)	AP	-34.9
(Cr*-Co)	AP	-47.9
(Mn*-Co)	AP	-45.4
(Mn*-Si*)	P	11.4
(Mn-Si)/Cr/(Mn-Si)	AP	-83.0
>(Mn-Co*)	AP	-90.5
>(Cr*-Si)	AP	-76.6
(Mn-Cr*)	AP	-82.5
(Co*-Si)	P	18.9
(Co-Co)/Cr/(Mn-Si)	P	58.8
(Cr*-Si)	P	56.5
(Mn-Co*)	P	67.3
(Mn-Cr*)	P	57.8
(Co*-Si)	AP	-14.4

It is basically possible to study the magnetic states in noncollinear alignments of the magnetization. We have tried it by incorporating the scalar relativistic effect into the PAW potential. However, we found that a self-consistent calculation is quite time consuming to obtain stable results. Therefore we will not mention the result in this paper.

IV. DISCUSSION

In the previous section, we presented the electronic and magnetic structures of Fe/Cr/Fe and CMS/Cr/CMS TLs calculated by the first-principles method. Here, we discuss the similarity and dissimilarity of Fe/Cr/Fe and CMS/Cr/CMS TLs, the effects of antisite atoms at interfaces on the magnetic structure, and a possible mechanism for the observed 90° coupling in CMS/Cr multilayers.

The tendency toward 90° coupling in Fe/Cr multilayers observed so far may be explained as follows. When a Cr layer is thin, its antiferromagnetic ordering vanishes, probably due to interfacial roughness, and the Cr layer becomes nonmagnetic, making the long-period oscillation dominant. In clean samples, however, antiferromagnetic ordering may survive and a short-period oscillation appears. Subject to ML steps at the interface, a frustration between P and AP alignments occurs, resulting in the 90° coupling.

The frustration may appear differently in CMS/Cr/CMS TLs when Cr moments are ordered antiferromagnetically. In the TLs, Mn moments align antiparallel to Cr moments at interfaces, whereas Co moments are parallel to Cr moments. As a result, the alignment of CMS magnetization in CMS/Cr/CMS depends on the combination of (Co-Co)/Cr and (Mn-Si)/Cr contacts at the interface. In a CMS/Cr/CMS TL with an even number of Cr MLs, P alignment occurs when two interfaces consist of different types of contact and AP

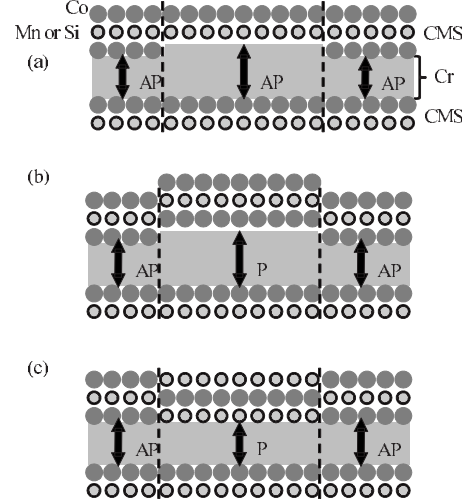


FIG. 10. IEC for (a) a step without antiphase structure, (b) a step with antiphase structure, and (c) an antiphase structure without steps.

alignment occurs when the same type of contact forms both interfaces. This indicates that the frustration may not appear even when a step exists at an interface, as Fig. 10(a) shows. The frustration of the magnetization alignment may occur when an antiphase structure exists, as Figs. 10(b) and 10(c) show. Note that the frustration appears even when no steps exist, as Fig. 10(c) shows.

We studied the effects of antisite atoms at interfaces on the magnetic structures in CMS/Cr/CMS TLs since the degree of order may not be 1.0 and some antisite atoms exist in CMS.^{39,40} Although a rich variety of structure is possible at the interface in CMS/Cr/CMS TLs, the trend of the magnetization alignment in TLs without antisite atoms, explained in the previous paragraph, could be preserved even in TLs with antisite atoms, with a few exceptions. In Fe/Cr/Fe, however, the effects of antisite Cr(Fe) on the magnetic structure of Cr and ΔE are rather strong, as shown in Fig. 3 and Table I. The difference in the results obtained for Fe/Cr/Fe and CMS/Cr/CMS TLs may affect the antiferromagnetic ordering in Cr layers; that is, the antiferromagnetic ordering of Cr moments might be more robust against roughness, such as antisite atoms at interfaces, in CMS/Cr/CMS TLs than in Fe/Cr/Fe TLs.

The argument above suggests a possible scenario for the 90° coupling in CMS/Cr multilayers: a robust antiferromagnetic ordering of Cr moments and a frustration caused by antiphase structures and/or step structures result in strong 90° coupling. Actually an effect of interface roughness on the exchange coupling was discussed for example by Costa *et al.*⁴¹

Finally, let us discuss IEC in terms of the J_1 and J_2 models given in Eq. (1) and the so-called proximity model,⁸ which is characterized by

$$E_{\text{ex}} = C_+ \{\theta\}^2 + C_- \{\pi - \theta\}^2. \quad (2)$$

It is known that the proximity model may be applied to multilayers in which the spacer layers are ordered antiferromag-

netically. Therefore, Eq. (2) may be more adequate than Eq. (1) to analyze experimental results of CMR/Cr/CMS multilayers. The main difference between Eqs. (1) and (2) is that a linear term in θ exists in the latter when θ is small. Since the torque $dE_{\text{ex}}/d\theta$ to rotate the magnetization alignment is non-zero for any θ in Eq. (2), this term yields an infinite saturation field in the magnetization of MLs. This tendency was clearly observed in CoFe/Mn/CoFe multilayers.⁴² Although the proximity model should be examined in detail, the experimentally derived conclusion that 90° coupling exists in CMS/Cr multilayers will be unchanged since the measurement of remanent magnetization is its main source. Comparison of the calculated ΔE with E_{ex} in Eqs. (1) and (2), however, is difficult at present because ΔE is much larger than E_{ex} .

V. CONCLUSION

We calculated the electronic structure, magnetic moments, and magnetic structures in Fe/Cr/Fe and CMS/Cr/CMS TLs with perfect interfaces as well as those with antisite atoms at interfaces by the first-principles method. For CMS/Cr/CMS TLs, we showed that the half-metallic character of CMS is lost at the interfaces and found that the Mn moments align

antiparallel to the Cr moment but the Co moments are parallel to the Cr moments at the interface. Because of the alignment of local moments at the interface, the sign of IEC in CMS/Cr/CMS TLs depends on the type of contact, (Co-Co)/Cr or (Mn-Si)/Cr, at the interfaces. The result indicates that a frustration of magnetization alignment is possible in multilayers with antiphase structure. The magnetization alignment and antiferromagnetic ordering of Cr moments in CMS/Cr/CMS multilayers are rather more robust against antisite atoms at the interface than those in Fe/Cr/Fe TLs. In view of these results, we suggested that the 90° coupling observed in CMS/Cr multilayers results from a combined effect of the robustness of the antiferromagnetic ordering of Cr moments and frustrations caused by roughness, antiphase structure, and/or steps.

ACKNOWLEDGMENTS

The authors thank S. Mitani, Y. Sakuraba, S. Bosu, and K. Takanashi for useful discussion and comments. The work was partly supported by the Next Generation Super Computing Project, Nanoscience Program, MEXT, Japan, Grants-in-Aids for Scientific Research in the priority area “Spin current” from MEXT, Japan, and Elements Science and Technology Projects of MEXT, Japan.

*Present address: ORDIST, Kansai University, Suita 564-8680, Japan.

†inoue@nuap.nagoya-u.ac.jp

¹P. Grünberg, R. Schreiber, Y. Pang, M. B. Brodsky, and H. Sowers, *Phys. Rev. Lett.* **57**, 2442 (1986).
²M. N. Baibich, J. M. Broto, A. Fert, F. Nguyen Van Dau, F. Petroff, P. Etienne, G. Creuzet, A. Friederich, and J. Chazelas, *Phys. Rev. Lett.* **61**, 2472 (1988).
³T. Miyazaki and N. Tezuka, *J. Magn. Magn. Mater.* **151**, 403 (1995).
⁴J. C. Slonczewski, *J. Magn. Magn. Mater.* **159**, L1 (1996).
⁵T. Marukame, T. Ishikawa, S. Hatamata, K. Matsuda, T. Uemura, and M. Yamamoto, *Appl. Phys. Lett.* **90**, 012508 (2007).
⁶T. Ishikawa, S. Hakamata, K. Matsuda, T. Uemura, and M. Yamamoto, *J. Appl. Phys.* **103**, 07A919 (2008).
⁷S. S. P. Parkin, N. More, and K. P. Roche, *Phys. Rev. Lett.* **64**, 2304 (1990).
⁸J. C. Slonczewski, *J. Magn. Magn. Mater.* **150**, 13 (1995).
⁹M. D. Stiles, in *Ultrathin Magnetic Structures III*, edited by J. A. C. Bland and B. Heinrich (Springer-Verlag, Berlin, 2005).
¹⁰D. M. Edwards and A. Umerski, in *Handbook of Magnetism and Advanced Magnetic Materials*, edited by H. Krummüller and S. S. P. Parkin (Wiley, New York, 2008).
¹¹B. Heinrich, in *Magnetic Heterostructures*, edited by H. Zabel and S. D. Bader (Springer-Verlag, Berlin, 2008), p. 185.
¹²D. M. Edwards, J. Mathon, R. B. Muniz, and M. S. Phan, *Phys. Rev. Lett.* **67**, 493 (1991).
¹³P. Bruno and C. Chappert, *Phys. Rev. Lett.* **67**, 1602 (1991).
¹⁴M. D. Stiles, *Phys. Rev. B* **48**, 7238 (1993).
¹⁵J. Unguris, R. J. Celotta, and D. T. Pierce, *Phys. Rev. Lett.* **67**,

140 (1991).
¹⁶S. T. Purcell, W. Folkerts, M. T. Johnson, N. W. E. McGee, K. Jager, J. aan de Stegge, W. B. Zeper, W. Hoving, and P. Grünberg, *Phys. Rev. Lett.* **67**, 903 (1991).
¹⁷M. Rühlig, R. Schäfer, A. Hubert, R. Mosler, J. A. Wolf, S. Demokritov, and P. Grünberg, *Phys. Status Solidi A* **125**, 635 (1991).
¹⁸B. Heinrich, J. F. Cochran, M. Kowalewski, J. Kirschner, Z. Celinski, A. S. Arrott, and K. Myrtle, *Phys. Rev. B* **44**, 9348 (1991).
¹⁹P. Grünberg, S. Demokritov, A. Fuss, R. Schreiber, J. A. Wolf, and S. T. Purcell, *J. Magn. Magn. Mater.* **104-107**, 1734 (1992).
²⁰A. Azevedo, C. Chesman, S. M. Rezende, F. M. de Aguiar, X. Bian, and S. S. P. Parkin, *Phys. Rev. Lett.* **76**, 4837 (1996).
²¹H. Wang, A. Saito, K. Saito, S. Mitani, K. Takanashi, and K. Yakushiji, *Appl. Phys. Lett.* **90**, 142510 (2007).
²²H. Wang, S. Mitani, A. Saito, K. Saito, K. Takanashi, and K. Yakushiji, *J. Appl. Phys.* **101**, 09J510 (2007).
²³S. Bosu, Y. Sakuraba, K. Saito, H. Wang, S. Mitani, and K. Takanashi, *IEEE Trans. Magn.* **44**, 2620 (2008).
²⁴S. Bosu, Y. Sakuraba, K. Saito, H. Wang, S. Mitani, K. Takanashi, C. Y. You, and K. Hono, *J. Appl. Phys.* **105**, 07C710 (2009).
²⁵S. Bosu, Y. Sakuraba, K. Saito, H. Wang, S. Mitani, and K. Takanashi, *Phys. Rev. B* **81**, 054426 (2010).
²⁶J. C. Slonczewski, *Phys. Rev. Lett.* **67**, 3172 (1991).
²⁷J. C. Slonczewski, *J. Appl. Phys.* **73**, 5957 (1993).
²⁸S. O. Demokritov, *J. Phys. D* **31**, 925 (1998).
²⁹S. Bosu, Ph.D. thesis, Tohoku University, 2009.
³⁰H. Hasegawa, *Phys. Rev. B* **42**, 2368 (1990).

- ³¹D. Stoeffler and F. Gautier, *J. Magn. Magn. Mater.* **104-107**, 1819 (1992).
- ³²D. Stoeffler and F. Gautier, *J. Magn. Magn. Mater.* **147**, 260 (1995).
- ³³S. Mirbt, A. M. N. Niklasson, B. Johansson, and H. L. Skriver, *Phys. Rev. B* **54**, 6382 (1996).
- ³⁴M. Freyss, D. Stoeffler, and H. Dreyssé, *Phys. Rev. B* **56**, 6047 (1997).
- ³⁵S. S. P. Parkin, *Phys. Rev. Lett.* **67**, 3598 (1991).
- ³⁶E. E. Fullerton, S. D. Bader, and J. L. Robertson, *Phys. Rev. Lett.* **77**, 1382 (1996).
- ³⁷K. Hirai, *J. Phys. Soc. Jpn.* **70**, 841 (2001).
- ³⁸K. Mibu, M. Almokhtar, S. Tanaka, A. Nakanishi, T. Kobayashi, and T. Shinjo, *Phys. Rev. Lett.* **84**, 2243 (2000).
- ³⁹S. Picozzi, A. Continenza, and A. J. Freeman, *Phys. Rev. B* **69**, 094423 (2004).
- ⁴⁰B. Hülsem, M. Scheffler, and P. Kratzer, *Phys. Rev. B* **79**, 094407 (2009).
- ⁴¹A. T. Costa, Jr., J. d'Albuquerque e Castro, and R. B. Muniz, *Phys. Rev. B* **59**, 11424 (1999).
- ⁴²M. E. Filipkowski, J. J. Krebs, G. A. Prinz, and C. J. Gutierrez, *Phys. Rev. Lett.* **75**, 1847 (1995).